Metallurgy and materials
Metalurgia e materiais

On the effect of interrupted ageing (T6I4) on the mechanical properties of AA6351 and AA7050 alloys

http://dx.doi.org/10.1590/0370-44672019740154

Ana Márcia Barbosa da Silva Antunes[1,3]
https://orcid.org/0000-0001-6856-2083
Carlos Antônio Reis Pereira Baptista[1,4]
https://orcid.org/0000-0001-5762-8235
Miguel Justino Ribeiro Barboza[1,5]
https://orcid.org/0000-0002-8367-358X
André Luís Moreira de Carvalho[2,6]
https://orcid.org/0000-0003-0086-7627

[1]Universidade de São Paulo – USP,
Escola de Engenharia de Lorena, Departamento de Engenharia de Materiais, Lorena - São Paulo – Brasil.

[2]Universidade Estadual de Ponta Grossa – UEPG,
Engenharia de Materiais,
Ponta Grossa – Paraná – Brasil.

E-mails: [3]anamarcia2359@gmail.com,
[4]baptista@demar.eel.usp.br, [5]miguelbarboza@usp.br,
[6]andrelmc@uepg.br

Abstract

The mechanical properties of age-hardenable aluminum alloys are strongly influenced by the volume fraction, size and spacing of hardening precipitates. In addition, researches have shown that interrupted ageing (T6I4) could benefit the hardening response of these alloys. Interrupted ageing is a term generally used for the microstructural development process of an alloy aged at a reduced temperature after partially aged at a higher temperature. Thus, this process produces a change in the mechanical properties of the alloy. In this study, the precipitate structures and mechanical properties of AA6351 and AA7050 alloys were investigated. Transmission electron microscopy analyses of the hardening precipitates were carried out. Hardness and tensile properties were performed to compare the effect of disrupted ageing on AA6351-T6 / AA6351-T6I4 and AA7050-T7451 / AA7050-T6I4 alloys. AA6351-T6I4 showed a higher volumetric fraction of hardening precipitates with heterogeneous size and resistance lower than AA6351-T6. In addition, AA7050-T6I4 showed a higher volumetric fraction of hardening precipitates with smaller size and similar resistance to AA7050-T7451. However, in both cases, interrupted ageing contributed to increase ductility and toughness.

Keywords: aluminum alloys; interrupted ageing; microstructure; mechanical properties.

1. Introduction

The 6xxx (Al–Mg–Si) and 7xxx (Al–Zn–Mg–Cu) series aluminum alloys are widely applied in the automotive and aircraft manufacturing due to their high strength to density ratio that allows the weight reduction of structures (Buha *et al*., 2008; Chen *et al*., 2013; Maeda *et al*., 2018). The changes in the aluminum alloys microstructure cause remarkable modifications in their properties (Souza *et al*., 2012). The hardening response of these alloys is substantially influenced by the size, shape and volume fraction of the hardening precipitates formed during ageing (Jiang *et al*., 2016). In addition, the hardening of these alloys increases with the amount of alloying elements by the modification of the microstructure (Mrówka-Nowotnik and Sieniawski, 2005). For example, the addition of 0.6% of copper to the 6082 Al–Mg–Si alloy increases the peak hardness as well as decreases the time to achieve the peak hardness (Man *et al*., 2007). Moreover, the addition of Ti combined with mechanical alloy also increased the hardness of the AA7050 alloy (Cardoso *et al*., 2007).

In fact, the precipitate structure control (size, shape and volume fraction) provided by the ageing treatments allows to achieve suitable combinations of properties for different applications. Therefore, investigations of hardening precipitates and hardening response of aluminum alloys resulting from different heat treatments, such as presented in this study, are essential to improve their selection and proper application. Taking this into account, several heat treatments have been developed for precipitation-hardenable aluminum alloys (Chen *et al*., 2013), including the interrupted ageing treatment (T6I4) (Risanti *et al*., 2009). In T6I4 treatment, "I" represents an interruption of the T6 condition by quenching and "4" is used to indicate ageing at ambient temperature or slightly higher (Lumley *et al*., 2002, Marceau *et al*., 2010).

Currently, several researches have shown that the interrupted ageing could improve the hardening response, and hence, the mechanical properties of some 6xxx and 7xxx series aluminum alloys (Buha *et al*., 2008; Risanti *et al*., 2009, Lima *et al*., 2014). Adoption of the T6I4 treatment may increase the volume fraction of hardening precipitates compared to the T7451 treatment in alloy AA7050, leading to an enhancement of fracture toughness without decrease of the tensile properties (Buha *et al*., 2008). For AA6061, the interrupted ageing treatment can also promote a

concurrent increase of toughness and strength (Lumley and Schaffer, 2006). However, for other aluminum alloys like 2090, 2091 and 8090, heat treatments with a low temperature step could decrease the mechanical properties as a consequence of the uncontrollable secondary precipitation (Lumley *et al*., 2002; Noble *et al*., 2006; Risanti *et al*., 2009). In this context, this study aims to evaluate mechanical properties and the possible relationship with the precipitate structure resulting from two different heat treatments of Al-Mg-Si AA6351 alloy (T6 and T6I4) and Al-Zn-Mg-Cu AA7050 alloy (T7451 and T6I4). The size and volumetric fraction as well as the distribution of the hardened precipitates were evaluated by transmission electron microscopy (TEM). It is worth to mention that these conditions of heat treatment were used in this investigation in order to verify the ability of the interrupted ageing to promote a better combination of mechanical properties of these alloys when compared to usual commercial conditions.

2. Experimental procedures

The AA6351 alloy was extruded to bars of 10×75 mm cross section at 400°C and the AA7050 alloy was hot rolled to 35 mm thickness plate at approximately the same temperature. These alloys were received in commercial tempers (solution treated and aged) conditions T6 and T7451, respectively, from which material samples were obtained to carry out the current study. The chemical composition of the AA6351 and AA7050 alloys used in this study were determined using optical emission spectrometry with Ametek Spectromaxx model LMF05 and Shimadzu PDA-700, respectively. The chemical compositions and the commercial heat treatments of the alloys are indicated in Table 1 and Table 2.

Table 1 - Chemical composition of the AA6351 and AA7050 alloys (wt%).

Alloy	Si	Fe	Cu	Zn	Mn	Mg	Cr	Zr	Ti
AA6351	1.01	0.191	0.103	-	0.482	0.373	0.0164	-	0.0303
AA7050	0.02	0.07	2.00	5.58	-	1.88	-	0.15	-

Table 2 - Heat treatment of the AA6351-T6 and AA7050-T7451 alloys.

Alloy/ Heat treatment	Treatment condition	Ageing	
		First step	Second step
AA6351-T6	10°C/min to 580°C 580°C - 15 min	180°C - 6 h	-
AA7050-T7451	10°C/min to 485°C 485°C - 4 h	110°C - 2 h	175°C - 10h

In order to achieve the T6I4 condition, the obtained rods (8 mm and length of 55 mm) were heat treated according to the parameters given in Table 3 (Risanti *et al*., 2009; Li *et al*., 2013; Buha *et al*., 2008; Lima *et al*., 2013; Lima *et al*., 2014).

Table 3 - Interrupted ageing treatment - AA6351 and AA7050 alloys.

Alloy/Ageing heat treatment	Treatment condition	Interrupted ageing	
		First step	Second step
AA6351/T6I4-65	560°C - 2 h	180°C - 1 h	65°C - 24 h
AA7050/T6I4-65	485°C - 3 h	145°C - 30 min	65°C - 24 h

The Vickers microhardness tests were performed in the longitudinal extrusion direction for the AA6351 alloy and in the longitudinal rolling direction for the AA7050 alloy. The adopted loads were 50 gf and 500gf, for AA6351 and AA7050 alloys respectively, while the indentation time was 15s for both cases. A Buehler Micromet 2004 equipment was employed in the tests and 20 measurements were made for each material condition.

TEM samples were obtained by cutting thin slices from the alloys. The slices were physically and mechanically-thinned down to 10 µm in a Gatan Disc Grinder Model 623 and Dimple Grinder Model 656.Thus, ion polishing of the samples was conducted by using a Gatan Precision Ion Polishing System (PIPS). The characterization of nanometric hardening precipitates was performed on a JEM 2100 transmission electron microscope at 200 kV. The average values of size and volume fractions of the hardening precipitates and intermetallic particles were verified by using the software IMAGE J 1.30. To obtain the average size of the nanometric hardening precipitates, 20 measurements of the precipitate size were performed using the software IMAGE J 1.30 for each of the conditions (AA7050-T7451, AA7050-T6I4, AA6351-T6 and AA6351-T6I4). The volumetric fractions of hardening precipitates was obtained by averaging the analyses of the obtained TEM images for each of the material conditions. The tensile tests were conducted on an EMIC electromechanical load frame model DL10000 at room temperature with a crosshead speed of 1 mm/min, according to the with ASTM E8/E8 M-11 Standard Test Method (ASTM, 2011).

3. Results and discussion

3.1 Hardening precipitates

Figure 1 (a) shows a TEM image of the AA6351-T6 alloy, where hardening precipitates with size of 169±53 nm can be seen in the Al matrix. Figures 1 (b) and (c) correspond to AA6351-T6I4 condition.

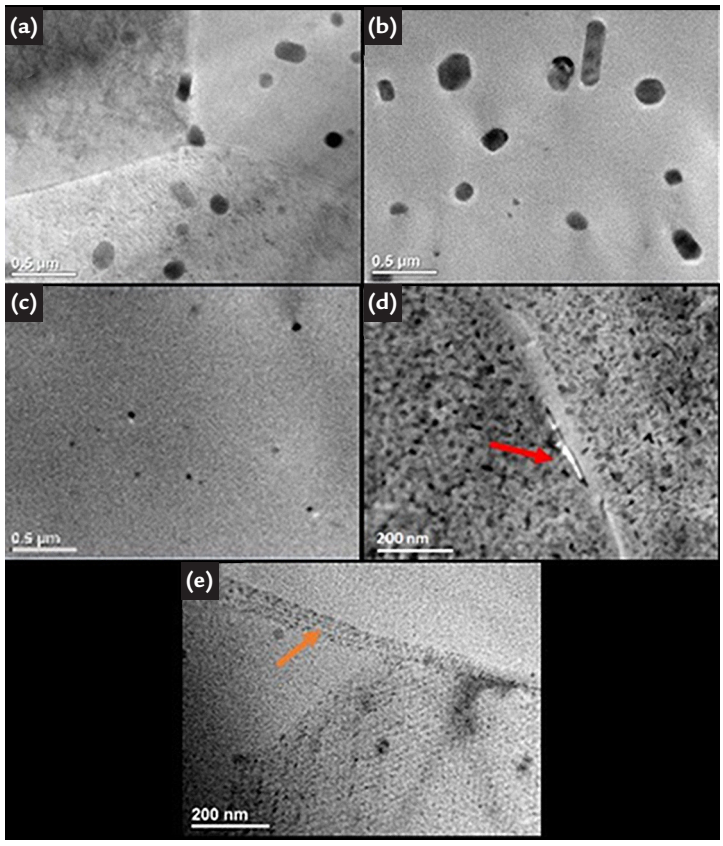

Figure 1 - TEM images of AA6351-T6 (a); AA6351-T6I4 (b-c); AA7050-T7451 (d) and AA7050-T6I4 (e).

The hardening precipitates shown in Figure 1 (b) have average size of 236±67 nm, consistent with precipitates β' size range (100 and 200 nm) in AA6351-T6I4 reported in (Fàre *et al*., 2011). Figure 1 (c) shows a specific region presenting smaller hardening precipitates with average size of 26±8 nm, and a discussion on the ageing conditions leading to this feature is presented as follows. Figure 1(d-e) shows intense precipitation with a homogeneous distribution within grains of hardening precipitates η in the AA7050-T7451 (Figure 1(d)) and GP zones and mainly η' in AA7050-T6I4 (Figure 1(e)) alloys.

The sequence of generic precipitation for the 6xxx series alloys is defined as: SSS (supersaturated solid solution) → AC → GP zones → β'' → β' + B' + U1+ U2 → β (Mg_2Si) phases (Murayama and Hono, 1999; Van Huis *et al*., 2006; Vissers *et al*., 2007; Son *et al*., 2011; Xiao-song *et al*., 2011; Simar *et al*., 2012; Maeda *et al*., 2018). In this sequence, initially, Mg and Si form atomic clusters (AC) and GP (Guinier-Preston) zones are originated (Vissers *et al*., 2007), with Si to Mg ratio close to 1 (Murayama and Hono, 1999). Upon additional ageing, β'' precipitates are formed (Vissers *et al*., 2007). These needle-like precipitates are the pivotal hardening phase in 6xxx alloys (Takeda *et al*., 1998), with size of ~4x4x50 nm (Andersen *et al*., 1998). Studies have shown that the sequence of precipitation in the Al-Mg-Si alloys is fairly complex. Except for the β phase (equilibrium phase), the stoichiometric ratio Mg_2Si is not observed. For example, Andersen *et al*., (1998) found that the β'' precipitate is constituted by Mg_5Si_6 phase. In addition, further studies carried out by Hasting *et al*., (2009) showed that the composition of the β'' precipitate includes Al and is composed of $Mg_5Al_2Si_4$ (Hasting *et al*., 2009). The β' precipitate (Mg_9Si_5 or Mg_6Si_3) is larger than its predecessor β'' and have been observed with size of approximately 100 and 200 nm (Gupta *et al*., 2001; Fàre *et al*., 2011). The equilibrium phase, β (Mg_2Si), is larger than other precipitates in 6xxx alloys, in shape of plates or cubes with length of several micrometers. The mentioned dimensions are only an approximate indication, since the actual values strongly depend on the heat treatment and composition of the alloy (Vissers *et al*., 2007).

In both heat treatment conditions studied in this research for the AA 6351 alloy, the precipitates are platelet or rod-shaped, identified as β' phase according to their morphology (Edwards *et al*., 1998; Gupta *et al*., 2001; Fàre *et al*., 2011; Rao *et al*., 2014). In AA6351-T6I4 condition, some regions were found (Figure (1c)) containing smaller spherical precipitates that on the base of their morphology were also identified as GP zones. These GP zones are resulting from the secondary precipitation that occurs during the second step of the interrupted ageing (65°C-24 hours) (Buha *et al*., 2007; Vissers *et al*., 2007).

The volume fractions of hardening precipitates are 3.4±0.8% and 5.7±2.2% for AA6351-T6 and AA6351-T6I4 conditions, respectively. These values were obtained by the analyses of

6 TEM images of each condition. Comparing to AA6351-T6, the AA6351-T6I4 alloy showed a slightly higher volume fraction of hardening precipitates and higher heterogeneity of the microstructure (indicated by the higher scatter of size of hardening precipitates and the volume fraction).

This higher heterogeneity of the microstructure in the AA6351-T6I4 could be originated by the coexistence of β' phase with the GP zones originated from the secondary precipitation in the second stage of the interrupted ageing. Also, the β' phase could coexist with precipitates of B' phase (ribbons up to 1 μm long constituted by $Al_3Mg_9Si_7$), U1 phase ($Mg_1Si_2Al_2$) and U2 phase ($Mg_4Si_4Al_4$), either needle-like precipitates with several hundred nanometers long, with ~15 nm diameter (Van Huis *et al*., 2006; Vissers *et al*., 2007). In addition, according to Buha *et al*., (2007), the first stage (at higher temperature) of the T6I4 treatment should be discontinued while the rate of nucleation is still higher than the hardening precipitates dissolution rate. Thus, if ageing is continued at a lower temperature during the second stage, as in the T6I4 treatment, a result is expected that indicates development of a higher density of hardening precipitates with smaller size (Buha *et al*., 2007). However, the AA6351-T6I4 condition presented a slightly higher volume fraction of hardening precipitates with higher average size. From this perspective, possibly the conditions of 1h at 180°C in the first step of the T6I4 treatment were not enough for the nucleation of every hardening precipitate that could grow during the second stage of the ageing, resulting in hardening precipitates with higher average size, as observed in the AA6351-T6I4 condition (Buha *et al*., 2007).

Indeed, previous studies of the AA7050-T7451 by using differential scanning calorimetry (DSC) showed that all the precipitates η' were transformed into η phase (Lima *et al*., 2013; Lima *et al*., 2014; Jacumasso, 2014). In both AA7050-T6I4 and AA7050-T7451 alloys, the η phase was found to have a larger size in the grain boundaries as shown in Figure 1 (e) (orange arrow) (Jacumasso, 2014).

In the 7xxx alloys, the sequence of precipitation is generally defined as: solid solution → G.P. zones → metastable η' → stable η ($MgZn_2$) (Du *et al*., 2006; Lin *et al*., 2006; Buha *et al*., 2008; Yang *et al*., 2015; Jiang *et al*., 2016; Lervik *et al*., 2020).

Firstly, Guinier Preston Zones (GP) are obtained from the supersaturated solid solution (SSS) (Lima *et al*., 2014). These GP zones behave as nucleation sites for η' precipitates (Yang *et al*., 2015). The η' phase has platelets morphology, and the heavy dispersion of this precipitate is associated with the optimum tensile properties of Al-Zn-Mg-Cu alloys (Hatch, 1984; Buha *et al*., 2008). The equilibrium phase η, $MgZn_2$, has different morphologies: plate shape or needle and is generated by the transformation from the η' phase. In addition, the η phase can present 9 different orientation relationships with aluminum matrix which are termed η_1 to η_9 (Buha *et al*., 2008).

The precipitates volume fraction is slightly higher in the AA7050-T6I4 (41.4±1.5 %), compared to AA7050-T7451 alloy (38.8±2.3 %). These values were obtained by the analyses of two TEM images of each condition by using the software Image J. In addition, the hardening precipitate sizes were of 30±12 nm and 5.5±1.7 nm for T7451 and T6I4 conditions, respectively.

It can be verified by comparing the Figures 1 (d) and (e) that AA7050-T6I4 condition resulted in a higher amount of hardening precipitates finely dispersed in the matrix. Thus, by reducing the ageing temperature in the second stage of the T6I4 heat treatment, most of the GP zones that were nucleated in the first step of the interrupted ageing were consumed in the η' phase formation. This increase in the η' precipitate density is correlated to the improved combination of mechanical properties in AA7050-T6I4 condition, compared to AA7050-T7451 (Buha *et al*., 2007; Buha *et al*., 2008; Feizi and Ashjari, 2018). In Figure 1 (d), a coarse intermetallic particle also can be observed along the grain boundary (red arrow) in the AA7050-T7451 condition. This coarse particle is probably constituted by Al_7Cu_2Fe phase (Jacumasso, 2014).

3.2 Hardness and tensile properties

Tables 4 and 5 shows Vickers hardness values and tensile properties obtained for AA6351-T6, AA6351-T6I4, AA7050-T7451 and AA7050-T6I4 alloys. Tensile properties were evaluated based on yield stress (σ_{ys}), ultimate tensile strength (σ_{UTS}), elongation to fracture (ε) and modulus of toughness (U_T). Additionally, Figure 2 presents the engineering stress-strain data curves for these alloys.

Table 4 - Vickers hardness values of AA6351 and AA7050 alloys.

Alloy/Condition	AA6351-T6	AA6351-T6I4	AA7050-T7451	AA7050-T6I4
Hardness (HV)	83.7 ± 4.4	65.3 ± 1.9	170 ± 2.7	171.0 ± 1.8

Table 5 - Tensile properties of AA6351 (T6 and T6I4) e AA7050 (T7451 and T6I4) alloys.

Alloy/conditions	σ_{YS} (MPa)	σ_{UTS} (MPa)	ε (%)	U_T (N mm/mm^3)
AA6351-T6	312	342	13	40
AA6351-T6I4	112	213	46	69
AA7050-T7451	470	531	11	52
AA6351-T6I4	473	561	19.4	100

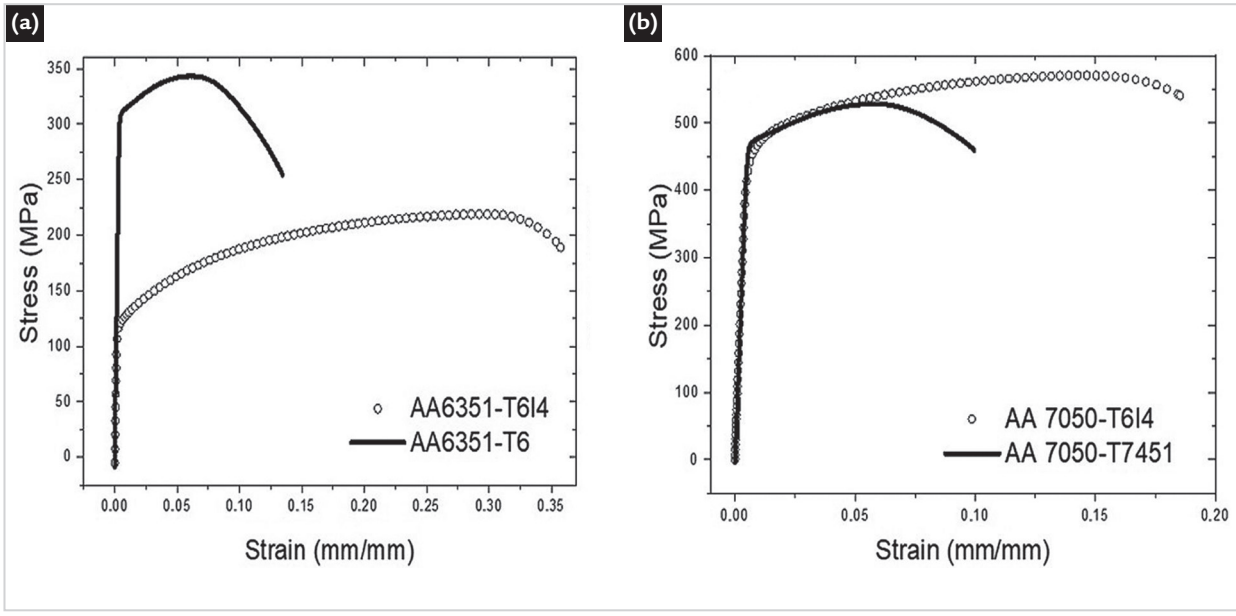

Figure 2 - Engineering stress–strain data curves for (a) AA6351-T6 and AA6351-T6I4; (b) AA7050-T7451 and AA7050-T6I4.

The Vickers hardness values of AA6351-T6I4 (65.3±1.9 HV) were lower when compared to the AA6351-T6 (83.7±4.4 HV) treatment. A reduction of approximately 22% was observed. Although it was expected that the T6I4 treatment could generate a higher density of hardening precipitates with smaller size and hence, a better hardening response (Buha *et al.*, 2007), this effect was not observed in the AA6351 alloy. The hardness values (Table 4) of AA7050-T7451 (170±2.7 HV) and AA7050-T6I4 (171.0±1.8 HV) conditions were similar. Based on the data in Table 5 and studies reported in (Antunes *et al.*, 2019) for AA7050 alloy, the interrupted ageing (T6I4) resulted in yield stress (σ_{ys}) and ultimate tensile strength (σ_{UTS}) comparable to the T7451 condition. However, there was an approximately 80% increase in elongation (ε) and 92% in modulus of toughness (U_T) due to T6I4 temper. For AA6351 alloy (Table 5), the T6I4 treatment contributed to a reduction of 64 and 38% in yield stress and ultimate tensile strength values, respectively. However, T6I4 increased ductility by up to 2.5 times and toughness modulus by approximately 73%. Therefore, 40% increase of β' precipitates size in AA6351-T6I4 contributed to resistance decrease and ductility increase. Although some areas on this alloy have shown smaller precipitates (GP zones), the second step of the interrupted ageing was more effective in the growth of pre-existing hardening precipitates rather than the nucleation of GP zones.

By the change in the η' phase size, at lower temperature ageing in the AA7050-T6I4, the process of nucleation was more effective than the growth, providing higher density of precipitates with reduced size, when compared to the T7451 condition. Therefore, the interrupted ageing heat treatment for the AA7050 alloy resulted in a precipitate hardening structure that is able to pin the dislocation motion as well as provide a higher deformation capacity of the material, and hence, increase its ductility without reducing the mechanical resistance.

4. Conclusion

This study presented results of the investigation on precipitates structure formed during treatment by interrupted ageing (T6I4) and mechanical properties of AA6351 and AA7050 alloys. The results were compared to the as-received conditions T6 and T7451, respectively.

For the AA6351-T6I4 condition, the interrupted ageing resulted in a heterogeneous microstructure due to the coexistence of β' phase, GP zones and B', U1 and U2 phases. The treatment increased average β' precipitates size by 40% contributing to resistance decrease and ductility increase.

The T6I4 condition resulted in a higher volume fraction of hardening precipitates of η' phase with a smaller size for the AA7050 alloy. It was also verified that the hardness, yield stress and ultimate tensile strength values were similar for AA7050-T7451 and AA7050-T6I4. Approximately 80% elongation increase and 92% in toughness due to the T6I4 temper has been observed.

In addition, although the interrupted ageing treatment is potentially beneficial to the microstructure and mechanical properties of aluminum alloys. Additional studies must be carried out with treatment time and temperature to obtain the best mechanical properties combination in AA6351 alloy.

Acknowledgements

The authors are thankful to CAPES and CNPq (Proc. 456808/2014-0) for the financial support to this research. Authors also thank PhD Naga Vishnu Vardhan Mogili, PhD Erico Teixeira Neto, PhD Carlos Alberto Ospina Ramirez and PhD Jefferson Bettini by the assistance in the TEM images acquisition. Research supported by LNNano - Brazilian Nanotechnology National Laboratory, CNPEM/MCTI.

References

AMERICAN SOCIETY FOR TESTING AND MATERIALS. ***ASTM E8 / E8M-11***: Standard test methods for tension testing of metallic materials. West Conshohocken, PA: ASTM, 2011. 27 p.

ANDERSEN, S. J.; ZANDBERGEN, H. W.; JANSEN, J.; TRAEHOLT, C.; TUNDAL, U.; REISO, O. The crystal structure of the β" phase in Al-Mg-Si alloys. ***Acta Materialia,*** v. 46, p. 3283-3298, 1998.

ANTUNES, A. M. B. S.; BAPTISTA, C. A. R. P.; BARBOZA, M. J. R.; CARVALHO, A. L. M.; MOGILI, N. V. V. Effect of the interrupted aging heat treatment T6I4 on the tensile properties and fatigue resistance of AA7050 alloy. ***Journal of the Brazilian Society of Mechanical Sciences and Engineering,*** v. 41, p. 1-13, 2019.

ASHJARI, M.; FEIZI, A. J. 7xxx aluminum alloys; strengthening mechanisms and heat treatment: a review. ***Material Science & Engineering International Journal,*** v. 2, n. 2, p. 49-53, 2018.

BUHA, J.; LUMLEY, R. N.; CROSKY, A. G. Secondary ageing in an aluminum alloy 7050. ***Materials Science and Engineering A,*** v. 492, p. 1-10, 2008.

BUHA, J.; LUMLEY, R. N.; CROSKY, A. G.; HONO, K. Secondary precipitation in an Al-Mg-Si-Cu alloy. ***Acta Materialia,*** v. 55, p. 3015-3024, 2007.

CARDOSO, K. R.; TRAVESSA, D. N.; ESCORIAL, A. G.; LIEBLICH, M. Effect of Mechanical Alloying and Ti Addition on solution and ageing treatment of an AA7050 aluminum alloy. ***Materials Research,*** v. 10, p. 199-203, 2007.

CHEN, Y.; WEYLAND, M.; HUTCHINSON, C. R. The effect of interrupted aging on the yield strength and uniform elongation of precipitation-hardened Al alloys. ***Acta Materialia,*** v. 61, p. 5877-5894, 2013.

DU, Z. W.; SUN, Z. M.; SHAO, B. L.; ZHOU, T. T.; CHEN, C. Q. Quantitative evaluation of precipitates in an Al-Zn-Mg-Cu alloy after isothermal aging. ***Materials Characterization,*** v. 56, p. 121-128, 2006.

EDWARDS, G. A.; STILLER, K.; DUNLOP, G. L.; COUPER, M. J. The precipitation sequence in Al-Mg-Si alloys. ***Acta Materialia,*** v. 46, p. 3893-3904, 1998.

FÀRE, S.; LECIS, N.; VEDANI, M. Aging behavior of Al-Mg-Si alloys subjected to severe plastic deformation by ECAP and cold asymmetric rolling. ***Journal of Metallurgy,*** v. 11, 2011.

GUPTA, A. K.; LOYD, D. J.; COURT, S. A. Precipitation hardening in Al-Mg-Si alloys with and without excess Si. ***Materials Science and Engineering A,*** v. 316, p. 11-17, 2001.

HASTING, H. S.; FROSETH, A. G.; ANDERSEN, S. J.; VISSERS, J. C. W. R.; MARIOARA, C. D.; DANOIX, F.; LEFEBVRE, W.; HOLMESTAD, R. Composition of β" precipitates in Al-Mg-Si alloys by atom probe tomography and first principles calculations. ***Journal of Applied Physics,*** v. 106, n. 123527, 2009.

HATCH, J. E. ***Aluminium***: properties and physical metallurgy. 2 ed. Ohio: Metals Park - American Society for Metals, 1984. 397p.

JACUMASSO, S. C. ***Caracterização microestrutural das partículas de segunda fase de uma liga de alumínio AA 7050 nas condições T7451, T6 e T6I4-65***. 2014. 112 f. Dissertação (Mestrado em Engenharia e Ciência dos Materiais) – Universidade Estadual de Ponta Grossa, Ponta Grossa, 2014.

JIANG, F.; ZUROB, H. S.; PURDY, G. R.; ZHANG, H. Characterizing precipitate evolution of an Al-Zn-Mg-Cu based commercial alloy during artificial aging and non-isothermal heat treatments by in situ electrical resistivity monitoring. ***Materials Characterization,*** v. 117, p. 47-56, 2016.

LERVIK, A.; MARIOARA, C. D.; KADANIK, M.; WALMSLEY, J. C.; MILKEREIT, B.; HOLMESTAD, R. Precipitation in an extruded AA7003 aluminium alloy: observations of 6xxx-type hardening phases. ***Materials and Design,*** v. 186, 108204, 2020.

LI, S.; HUANG, Z.; CHEN, W.; LIU, Z.; QI, W. Quench sensitivity of 6351 aluminum alloy. ***Trans. Nonferrous Met. Soc. China,*** v. 23, p. 46-52, 2013.

LIMA, L. O. R.; JACUMASSO, S. C.; CARVALHO, A. L. M. Influence of secondary ageing on mechanical properties of an AA7050 aluminum alloy. In: INTERNATIONAL CONGRESS ON THE MECHANICAL ENGINEERING, 22., Ribeirão Preto, 2013. ***Proceedings*** […]. Ribeirão Preto: COBEM, 2013. p. 7263-7270.

LIMA, L. O. R.; JACUMASSO, S. C.; RUCHERT, C. O. F. T.; MARTINS, J. P.; CARVALHO, A.L.M. Study of the effects of two-step ageing heat treatment on fatigue crack growth on an AA 7050 aluminum alloy. ***Advanced Materials Research,*** v. 891, p. 1111-1116, 2014.

LIN, J. C.; LIAO, H. L.; JEHNG, W. D.; CHANG, C. H.; LEE, S. L. Effect of heat treatments on the tensile strength and SCC-resistance of AA7050 in an alkaline saline solution. ***Corrosion Science,*** v.48, p. 3139-3156, 2006.

LUMLEY, R. N.; MORTON, A. J.; POLMEAR, I. J. Enhanced creep performance in an Al-Cu-Mg-Ag alloy through underageing. ***Acta Materialia,*** v. 50, p. 3597-3608, 2002.

LUMLEY, R. N.; POLMEAR, I. J.; MORTON, A. J. Control of secundary precipitation to improve the performance of aluminium alloys. ***Materials Science Forum,*** v. 396, p. 893-898, 2002.

LUMLEY, R. N.; SCHAFFER, G. B. Precipitation induced densification in a sintered Al-Zn-Mg-Cu alloy. ***Scripta Materialia,*** v. 55, p. 207-210, 2006.

MAEDA, T.; KANEKO, K.; NAMBA, T.; KOSHINO, Y.; SATO, Y.; TERANISHI, R.; ARUGA, Y. Structural and compositional study of precipitates in under-aged Cu added Al-Mg-Si alloy. ***Scientific Reports,*** v. 8, 2018.

MAN, J.; LI JING, L.; JIE, S. G. The effects of Cu addition on the microstructure and thermal stability of an

Al-Mg-Si alloy. ***Journal of Alloys and Compounds,*** v. 437, p. 146-150, 2007.

MARCEAU, R. K.W.; SHA, G.; LUMLEY, R. N.; RINGER, S. P. Evolution of solute clustering in Al-Cu-Mg alloys during secondary ageing. ***Acta Materialia,*** v. 58, p. 1795-1805, 2010.

MRÓWKA-NOWOTNIK, G.; SIENIAWSKI, J. Influence of heat treatment on the microstructure and mechanical properties of 6005 and 6082 aluminum alloys. ***Journal of Materials Processing Technology,*** v. 58, p. 312-317, 2005.

MURAYAMA, M.; HONO, K. Pre-precipitate clusters and precipitation processes in Al-Mg-Si alloys. ***Acta Materialia,*** v. 47, p. 1537-1548, 1999.

NOBLE, B.; HARRIS, S. J.; KATSIKIS, S.; DINSDALE, K. Low temperature stability of quartenary Al-Li-Cu-Mg--Alloy. ***Materials Science Forum,*** v. 519, p. 209-214, 2006.

RAO, P. N.; VISWANADH, B.; JAYAGANTHAN, R. Effect of cryorolling and warm rolling on precipitation evolution in Al 6061 alloy. ***Materials Science and Engineering A,*** v. 606, p. 1-10, 2014.

RISANTI, D. D.; YIN, M.; CASTILHO, P. E. J. R. D.; ZWAAG, S. V. D. A systematic study of the effect of interrupted ageing conditions on the strength and toughness development of AA6061. ***Materials Science and Engineering A,*** v. 523, p. 99-111, 2009.

SIMAR, A.; BRÉCHET, Y.; MEESTER, B.; DENQUIN, A.; GALLAIS, C.; PARDOEN, T. Integrated modeling of friction stir welding of 6xxx series Al alloys: Process, microstructure and properties. ***Progress in Materials Science,*** v. 57, p. 95-183, 2012.

SON, S. K.; MATSUMURA, S.; FUKUI, K.; TAKEDA, M. The compositions of metastable phase precipitates observed at peak hardness condition in an Al-Mg-Si alloy. ***Journal of Alloys and Compounds,*** v. 509, p. 241-245, 2011.

SOUZA, F. M.; LIMA, N. B.; PLAUT, R. L.; FERNANDES, R. C.; PADILHA, A. F. A comparative study in AA4006 alloy strips produced by twin roll caster and direct chill processes: microstructure and crystallographic texture. ***REM - Revista Escola de Minas,*** v. 65, n. 2, p. 205-216, 2012.

TAKEDA, M.; OHKUBO, F.; SHIRAI, T.; FUKUI, K. Stability of metastable phases and microstructures in the ageing process of Al-Mg-Si ternary alloys. ***Journal of Materials Science,*** v. 33, p. 2385-2390, 1998.

VAN HUIS, M. A.; CHEN, J. H.; ZANDBERGEN, H. W.; SLUITER, M. H. F. Phase stability and structural relations of nanometer-sized, matrix-embedded precipitate phases in Al-Mg-Si alloys in the late stages of evolution. ***Acta Materialia,*** v. 54, p. 2945-2955, 2006.

VISSERS, R.; VAN HUIS, M. A.; JANSEN, J.; ZANDBERGEN, H. W.; MARIOARA, C. D.; ANDERSEN, S. J. The crystal structure of the β' phase in Al-Mg-Si alloys. ***Acta Materialia,*** v. 55, p. 3815-3823, 2007.

XIAO-SONG, J.; GUO-QIU, H.; BING, L.; SONG-JIEL, F.; MIN-HAO, Z. Microstructure-based analysis of fatigue behavior of Al-Si-Mg alloy. ***Trans Nonferrous Met Soc China,*** v. 21, p. 443-448, 2011.

YANG, W.; JI, S.; ZHANG, Q.; WANG, M. Investigation of mechanical and corrosion properties of an Al-Zn-Mg-Cu alloy under various ageing conditions and interface analysis of η′ precipitate. ***Materials and Design,*** v. 85, p. 752-761, 2015.

Received: 29 November 2019 - Accepted: 24 August 2020.